



*Citation for published version:*

Costa, E, Oval, R, Shepherd, P & Orr, J 2023, 'Computational design exploration of a segmented concrete shell building floor system', *Proceedings of the Institution of Civil Engineers-Structures and Buildings*.  
<https://doi.org/10.1680/jstbu.22.00156>

*DOI:*

[10.1680/jstbu.22.00156](https://doi.org/10.1680/jstbu.22.00156)

*Publication date:*

2023

*Document Version*

Peer reviewed version

[Link to publication](#)

*Publisher Rights*

CC BY

The final publication is available at ICE publishing via <https://doi.org/10.1680/jstbu.22.00156>

**University of Bath**

**Alternative formats**

If you require this document in an alternative format, please contact:  
[openaccess@bath.ac.uk](mailto:openaccess@bath.ac.uk)

**General rights**

Copyright and moral rights for the publications made accessible in the public portal are retained by the authors and/or other copyright owners and it is a condition of accessing publications that users recognise and abide by the legal requirements associated with these rights.

**Take down policy**

If you believe that this document breaches copyright please contact us providing details, and we will remove access to the work immediately and investigate your claim.

# Computational design exploration of a segmented concrete shell building floor system

## Abstract

The construction industry is responsible for nearly half of the UK's carbon emissions, and the use of an extremely large volume of concrete, the world's most widely used man-made material, accounts for more than 7% of global CO<sub>2</sub> emissions.

The scale of this problem spawned research that explored the potential for structurally efficient non-prismatic geometries to substantially reduce the amount of concrete in building elements, thus also reducing their embodied carbon footprint. In particular, the research focused on segmented thin concrete shells as floor slabs, leveraging computational design and digital fabrication methodologies to automate their production off-site.

An important part of this research was the development of a computational framework for the design of thin concrete shells, to make such construction methodology accessible to building designers in practice. The framework combined solutions for parametric modelling, finite element analysis, isogeometric analysis, form finding and optimisation, and also embedded fabrication constraints specific to the project's automated manufacturing system.

This paper documents the application of the developed computational framework in the design of a 4.5m x 4.5m prototype, illustrating how automating concrete construction can transform the industry towards net-zero.

**Keywords:** computational design; digital fabrication; concrete structures; shells; finite-element modelling, UN SDG 12: Responsible Consumption and Production, UN SDG 13: Climate Action

## 1 Introduction

The construction industry is responsible for nearly half of the UK's carbon emissions (Department for Business Innovation & Skills, 2010) and the use of an extremely large volume of concrete, the world's most widely used man-made material, accounts for more than 7% of global CO<sub>2</sub> emissions (Anderson and Moncaster, 2020).

Traditional formwork methods for concrete result in prismatic building elements (such as beams, floors slabs and columns), not because such shapes are needed for efficient load bearing, but because existing fabrication techniques rely on easy-to-construct prismatic moulds. Research has shown that up to 50% of the concrete in traditionally built elements is there only because of the prismatic formwork it was made in, and could be removed (Orr et al., 2011). For too long, the industry has used "ease of construction" as an excuse to waste material.

The scale of this problem spawned a research project, titled "Automating Concrete Construction" (ACORN), that explored the potential for structurally efficient non-prismatic geometries to

substantially reduce the amount of concrete in building elements, thus also reducing their embodied carbon footprint. These objectives align with the United Nations' Sustainable Development Goals (United Nations, 2015), in particular with SDG 12 related with Responsible Consumption and Production, and SDG 13 related with Climate Action (Opon and Henry, 2019). In particular, this project focused on segmented thin concrete shells as floors, leveraging computational design and digital fabrication methodologies to automate their production (Shepherd et al., 2019).

Floor slabs represent more than half of the structural mass of a building (De Wolf et al., 2016). Previous research has shown that thin concrete shells are a feasible alternative to flat slabs, yielding considerable reductions above 50% in both embodied carbon and self-weight (Block et al., 2020; Hawkins et al., 2020). Slabs rely on bending to carry loads, which requires thickness and reinforcement due to tensile forces. On the other hand, shells rely mainly on membrane action, thanks to their curvature, with their supports providing horizontal reaction through external thrust or internal ties. While the architectural qualities of vaulted floors have been explored and demonstrated over time (Bannister, 1968; Block et al., 2010; Guastavino, 1892), the use of thin shells for building floors raises engineering questions related to structural performance, but also to acoustics (Broyles et al., 2022) and current fire safety regulations – even though one of the main drivers for the early adoption of vaulted flooring in the 19<sup>th</sup> century was its fireproof quality (Ochsendorf and Freeman, 2014). Perhaps more significantly, there are construction challenges to be considered, related to how these structures can be efficiently fabricated and assembled, justifying the integration of these challenges in design exploration.

This paper documents the application of the developed computational framework for design exploration of a full-scale, 4.5m x 4.5m prototype of the segmented shells, called 'OAK' (Figure 1), whose fabrication is explored in depth by Oval et al. (2023). These two papers illustrate how automating concrete construction can help drive the industry towards net-zero.



Figure 1 – Left: Render of assembled ACORN thin-shell floor system; Right: Shell standing once assembled on columns with a levelled floor. Photo credit: ©John Orr

Section 2 addresses the coordination between design and digital fabrication. Section 3 provides an overview of the digital design tool, implemented as a Grasshopper plugin for the software Rhino3D, addressing the different aspects of the design process for the OAK shell prior to, but informed by, its fabrication, namely the geometrical modelling and the structural modelling. Section 4 presents the design exploration leading to the final OAK design and features a discussion of results.

## 2 Construction-aware design

The demonstrator prototype OAK was produced at the National Research Facility for Infrastructure Sensing (NRFIS) of the University of Cambridge. The design resulted from an exploration process enabled by a parametric design framework developed for the ACORN project, informed by architectural, structural and construction requirements, including building integration, fabrication, transport, assembly, and resource reuse.

### 2.1 Architectural requirements

The demonstrator included the concrete shell, steel columns as vertical supports, steel tie-rods to counteract the horizontal thrust, and a raised floor for accessibility, below which building services could be integrated, as shown in Figure 2.

The OAK shell has a span of 4.5m, covering a square area of 20m<sup>2</sup>, and a maximum rise of 590mm at the apex. The shell was form-found to behave mainly in compression, with uniform stresses resulting in a dome-like shape. Its thickness increases from 30mm at the apex to 60mm at the supports, and a set of ribs stiffen and strengthen the shell, by creating a local thickness of 60mm across a width of 300mm.

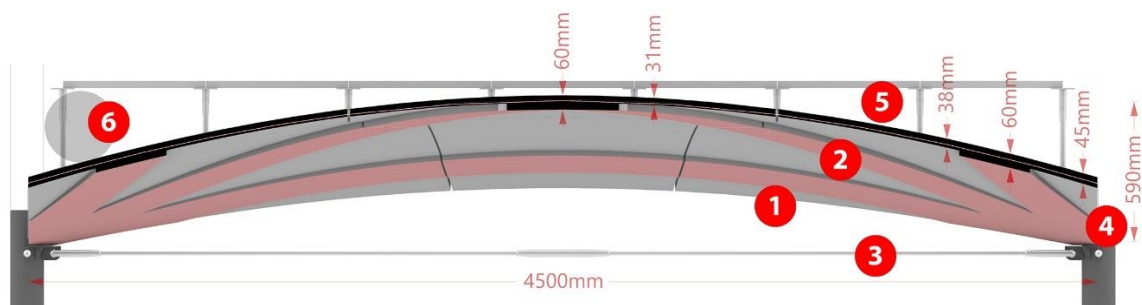


Figure 2 – Cross section through shell's apex: 1 - segmented shell; 2 - shell ribs (in red); 3 - tie rods; 4 - column heads; 5 - raised floor; 6 – space for Ø300 mm duct

### 2.2 Construction requirements

The proposed shells are to be produced off-site, in order to benefit from the precision and controlled environment of a manufacturing plant, which leverages automation and minimises waste, aiming for reducing the environmental impact by limiting construction waste in casting and formwork. The OAK shell was assembled close to where the segments were fabricated, at NRFIS. However, off-site production poses logistic constraints for a monolithic floor, related to fabrication, transportation, and assembly, which require the shell to be subdivided into transportable segments that are stacked for transportation and can be assembled on-site (Figure 3, right).



Figure 3 – Reconfigurable mould actuated by a set of vertical mechanically driven pins and connecting flexible formwork (left) and prefabricated segments ready to be transported and assembled (right). Photo credit: ©Robin Oval

To enable a circular economy of construction, the joints between the segments are dry – without mortar or grout – and thus reversible for disassembly. Rubber-lined half-joint shear keys prevent out-of-plane sliding failure in the direction where the compression forces in the shell induce shear at the interfaces. The keys are interrupted before the extremities of the interfaces, to avoid overlaps, and to provide additional in-plane interlocking between the segments (Figure 4).

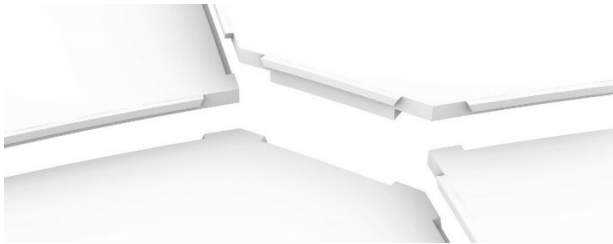


Figure 4 – Exploded view of the connections centred on the interface between shell segments. Image credit: ©Robin Oval

Production of the segmented shells relies on the innovative articulation of fabrication technologies, which include a reconfigurable mould system for defining the shell’s casting surface and robotic concrete spraying for producing the shell (Nuh et al., 2022; Oval et al., 2021). The reconfigurable mould system used in ACORN actuates a flexible formwork for shaping the concrete shell. It consists of a set of four 1m x 1m modules, which can be laid out into a larger 2m x 2m mould, used to fabricate shell segments (Figure 3, left). The mould is completed by a flexible formwork supported by the grid of actuated pins. The flexible formwork consists of an array of carbon strips, covered with a textile membrane, commonly used for flexible formwork (Hawkins et al., 2016). Initial physical experiments suggested limiting the size of each segment to fit a 1.8m-sided square, a constraint driven by the size of the mould and the low stiffness of the cantilevering part of the flexible formwork. This is a stronger constraint than the one due to factory-to-site transportation, which would allow for segments up to 12m x 3m (Liew et al., 2019).

For the shell itself, concrete is cast on the formwork using a robotic spraying system. To tackle the need for a ductile behaviour, short fibres are added to the sprayed concrete.

### 2.3 Structural requirements

Structural performance has been the main consideration when designing the segmented shell, since it informs not only the shell’s integrity but also its efficiency in terms of concrete volume. Therefore, its design is subjected to finite element (FE) analysis to simulate and quantify its structural behaviour

against three criteria: strength, informed by principal stresses; stability, informed by buckling load factors; and serviceability, informed by deflection.

Structural behaviour is assessed via a linear elastic analysis, using second-order theory to account for the effect of compression forces on stiffness, which therefore enables to calculate buckling. The use of such a simpler linear model enables design exploration, form finding and optimisation by significantly reducing computation time compared to a more refined non-linear analysis. On the other hand, geometrical (increase in deformations) and material (decrease in strength) non-linearities are not considered in this model, even though ignoring them leads to an overestimate of the buckling resistance, and therefore further development should take them into account.

**Strength** The criterion for evaluating the strength of an ACORN shell is informed by principal stress ( $\sigma$ ) values of every element of the shell's FE model. These values correspond to both  $\sigma_1$  and  $\sigma_2$ , measured both on the shell's top and bottom surfaces. Preliminary FE analyses resulted in stress concentrations occurring at the shell-column interface at the corners. However, previous research shows that such peak stresses are dependent on mesh size and artefacts, and that the plastic behaviour of GFRC is expected to redistribute such peak stress (Hawkins, 2020). Therefore, a percentage of the extreme  $\sigma$  values of the set was discarded, and the highest values of the remaining set would be considered. While such percentage can be defined by the user, in the case of the OAK prototype it was set to 5%, determined during development of the analysis framework by inspecting the location of elements with extreme  $\sigma$  values. Therefore, the shell strength indicator considered for design decisions was the 95-percentile Principal Stress. The maximum compressive  $\sigma$  value admitted by the material was set to 20 MPa, corresponding to the design compressive strength of C30/37 concrete ( $f_{cd} = \alpha_{cc} f_{ck} / \gamma_c$ ), using a partial safety factor  $\gamma_c = 1.5$  according to BS EN 1992-1-1 Eurocode 2 (British Standards Institution, 2004) While compression  $\sigma$  was considered to be the driving factor given the compression-dominant nature of the shell, tension principal stress is also measured and compared against a maximum value of 4.0 MPa.

**Stability** ACORN shells are cast on a flexible formwork, with which imperfections are higher than if cast on a rigid formwork. Indeed, shells in compression, specifically shallow shells with a low curvature, are particularly sensitive to shape imperfections, which render buckling critical (Medwadowski, 2004; Reitingner and Ramm, 1995). Therefore, buckling was considered essential to assess structural behaviour. For design exploration purposes, a minimum buckling load factor of 10 was determined to be the threshold value. Such a high safety factor is justified by the use of a simplified linear structural model, which leads to an overestimation of the buckling resistance (Hawkins et al., 2020).

**Serviceability** Deflection values were also calculated and deemed acceptable for a span/deflection ratio greater than 200. Usually critical for the design of flat slabs, the high stiffness of compression shells yields low deflections that are not determinant for design.

### 3 Computational design framework

The design process of OAK was facilitated by a computational design tool developed for the ACORN project, whose goal is to drive designers towards adopting non-prismatic concrete elements in their building designs (Costa et al., 2021). Focusing on thin concrete shells, the design tool is supported by an automated design framework composed of parametric tools, which integrates Grasshopper (GH) for Rhinoceros3D v1.0.0007 (Rutten, 2009), structural finite element analysis (FEA) plugin Karamba3D v1.3.3 (Preisinger, 2013) and iso-geometric analysis (IGA) plugin Kiwi!3D v0.5.0 (Längst et al., 2017). The resulting design tool is implemented as a GH plugin under the working title 'SQUIRREL'.

Additionally, a custom tool was developed for Design Space Visualisation (DSV), which is implemented as an extension of the Design Space Exploration (DSE) plugin for Grasshopper (Brown et al., 2020), and integrated in SQUIRREL. DSV automates the generation of multidimensional design and objective spaces and the plotting of two- and three-dimensional graphs from those spaces within Grasshopper, removing the need for additional external software typically used for this purpose, such as MATLAB, which would interrupt the continuous workflow needed for design exploration.

The implemented framework enables the assembly of a comprehensive parametric model of the ACORN shell, comprising a geometrical representation and a corresponding structural representation, along with a set of assessment tools. These tools generate efficient shapes through a form finding process, analyse the model's structural performance in near real-time, check its compliance with fabrication constraints, and visualise its shape prior to construction. While such workflow is focused on a specific construction technique, the ACORN approach could be integrated into existing Building Information Modelling (BIM) software and interoperability platforms through further development.

### 3.1 Geometrical model

The shell design process begins by defining its initial geometry, in particular by determining its floor plan. In a typical building design process, the slab size is defined by the column grid and subsequent bay geometry. Corners are chamfered from the initial floor plan, resulting in corner edges that account for the interface between the shell and the columns.

The shell's three-dimensional shape is then defined through form finding, a process commonly used in structural design to find efficient shapes in equilibrium, being particularly useful in exploring the design of shells with a dominant load case (Goldbach et al., 2020). ACORN's form finding process uses Kiwi!3D (Kiwi), which uses NURBS geometry as an input for isogeometric structural analysis, as opposed to a polygonal mesh which is the geometry required by FEA like Karamba, avoiding possible inaccuracies derived from converting NURBS to mesh (Bauer et al., 2017). Moreover, being Rhinoceros's native geometry type, maintaining the geometry as NURBS allows for a wider range of design operations like segmentation. Subsequent structural analysis tasks are performed using Karamba, since it provides a considerably wider range of outputs than Kiwi. The process uses Kiwi's 'Formfinding' implementation, which is based on the Updated Reference Strategy and suited to modelling the behaviour of tensile structures such as membranes (Bletzinger and Ramm, 1999). In this case, a membrane tensile structure is used to find a tension-only funicular shape, which is then inverted vertically to give a compression-only shell, by extension of the so-called Hooke's inversion (Robert Hooke, 1675). For this purpose, the shell plan geometry is translated into a Kiwi structural model containing information about structural elements, supports and loads (Figure 5).

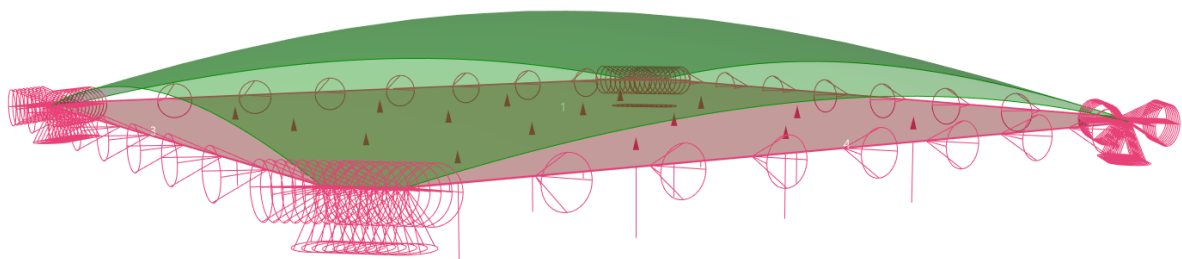


Figure 5 – Flat Kiwi structural model for formfinding (in pink color): cones correspond to constrained degrees of freedom at supports, arrows correspond to the uniformly distributed load; resulting surface in green color.

For the Kiwi model, the chamfered square shell plan is converted into a planar NURBS surface and used as a single membrane structural element. The membrane is assigned Kiwi's default ETFE material, with default material stiffness of 1 GPa, thickness of 1mm, surface refinement factor of 15 and surface

stress of 0.335 kN/m in both directions. The lines that connect the chamfered corners are converted into structural cables, enabling a more precise control of the shell's shape at the edges. The cables are assigned Kiwi's default steel material, with default material stiffness of 210 GPa, diameter of 10 mm, curve refinement factor of 8, and an edge force of 0.915 kN. Note that even though specific values are needed for assembling the Kiwi digital model, including material properties, forces and stresses, these do not have a meaningful correspondence with the actual material used in producing the shell. Nevertheless, they are included in this paper for reproducibility purposes. Moreover, refinement factors are dimensionless since they pertain to the number of subdivisions in NURBS curves and surfaces.

Both surface stress and edge force values are used to manipulate the resulting shape. A higher edge force flattens down the shell's edge, resulting in a more dome-like shape, whereas a higher surface stress makes the shell flatter around the apex and with a more pronounced slope at the corners (see Table 1 in the next section on Design Exploration).

The chamfered corners are divided into sets of eight points and encoded into the structural model as pinned supports, restrained in all three directions but free to rotate. The lines converted to cables are also divided into sets of eight points and encoded as supports in which only translation in the horizontal direction perpendicular to the edge is restrained (Figure 5). This counters the membrane's tendency to pull itself inwards due to surface stress, ensuring that the shell's sides are kept within a vertical plane. A uniformly distributed load of 0.1 is applied in the upward vertical direction. Finally, the deformation is adjusted by scaling deflections to match a target height, defined as an initial parameter of the design workflow.

The resulting membrane is form found to behave mainly in tension when subjected to the applied upward uniform load, which corresponds to inverting the primary loading of the ACORN floor. Inverting the load vertically results in a shell behaving mostly in compression, with a relatively uniform stress state, resulting in a dome-like shape with positive double curvature everywhere.

### 3.2 Structural model

The shell's geometrical model is converted into a structural model that can be computed by Karamba3D (K3D), enabling it to perform structural analyses using K3D's implementation of a second-order linear elastic model, through an iterative procedure with repeated updates of second order normal forces acting on the shell (Preisinger and Tam, 2020). ACORN K3D models are assembled from specific inputs that include structural shell elements, supports, cross sections, materials, and loads.

**Shell segments** In a K3D model, the ACORN shell segments correspond to a set of nine shell elements, each defined by a mesh, which derives from the shell's mid-surface, and a thickness distribution, both of which are informed by the geometrical model. Since K3D implements FEA, such mid-surface is represented by a polygonal mesh (Debney, 2020), rather than a NURBS surface, which is the type of geometry adopted to represent the shell shape in the preceding form-finding model. Through mesh convergence analysis, the mesh size selected for the structural model has an average edge length of 40mm, corresponding to 90% of the average thickness of the shell's final design, and totals 26k faces.

**Supports** The structural model comprises four sets of support points, one set for each corner. These supports are oriented in the direction of the corner edge, with unconstrained rotation about all axes. Translation is unconstrained along the corner edge, and is fixed in the vertical Z axis, corresponding to the column's reaction force countering gravity, and in the direction perpendicular to the edge towards the inside of the shell, corresponding to the reaction force countering the shell's thrust (Figure 6, left).



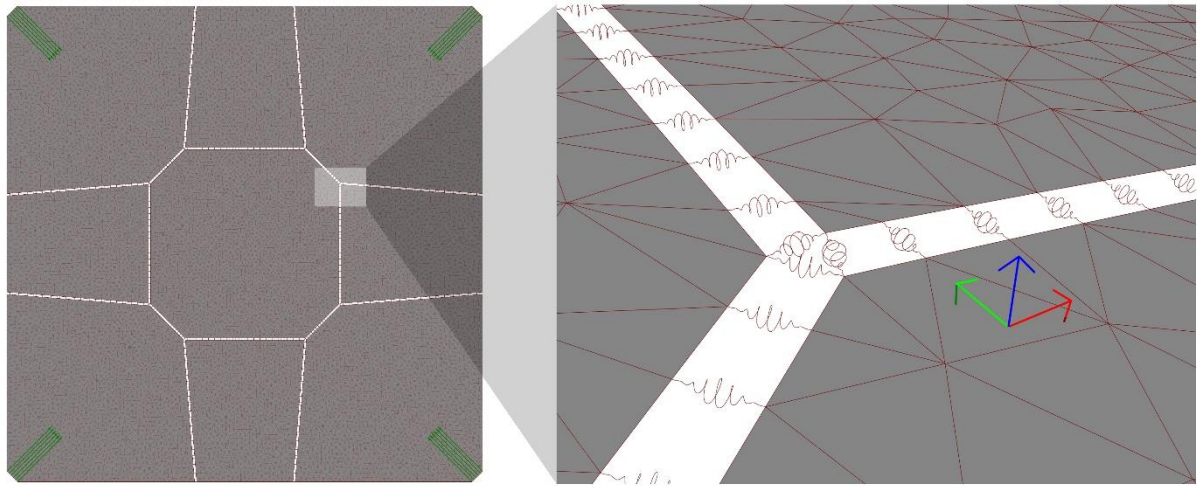


Figure 6 – Left: Oriented supports (green) in the K3D structural model; Right: Detail of segment interfaces, with local coordinate systems per spring (X in red, Y in green, Z in blue)

**Interfaces between segments** In the K3D model, the interface between any pair of segments is modelled as a set of springs distributed along their shared edge, connecting neighbouring vertices between corresponding segments meshes. In terms of K3D, such springs are implemented as beam elements characterised by a cross section of the type ‘Spring’, which is defined directly by translational and rotational stiffness values in its three local directions, determined through comparison with an unsegmented shell model. The spring cross section used in the segmented shell features high translational stiffness  $C_t=10^7$  kN/m in all three directions, corresponding to the locking action between segments resulting from compression and the shear keys. In terms of rotation, a low rotational stiffness  $C_r=0.01$  kNm/rad was assigned around the Z direction (in green in Figure 6, right), corresponding to the direction of the edge shared between segments, whereas the remaining two directions feature high rotational stiffness  $C_r=1000$  kNm/rad, derived from the locking action of the dry joints. This means that the segments are tied together but can fold along their shared edge without transferring bending moments.

**Material** In preliminary design stages, the theoretical material considered in the structural model corresponded to K3D’s predefined concrete C45/55, with stiffness  $E=36$  GPa, compressive strength  $f=30$  MPa and specific weight  $\gamma=25$  kN/m<sup>3</sup>. As fabrication efforts progressed, material properties of the structural model were updated to reflect preliminary results from compression and bending tests performed on samples of the concrete being used on the prototypes and the actual OAK shell. The tested material corresponds to compression stiffness  $E_{\text{comp}}=30$  GPa, bending stiffness  $E_{\text{bend}}=20$  GPa, compressive strength  $f_c=43$  MPa, tensile strength  $f_t=7$  MPa, and specific weight  $\gamma=20$  kN/m<sup>3</sup>. This updated information was used in analysing the behaviour of the shell after its design had been determined.

**Loadcases** The load cases included self-weight  $G$ , dead load  $G'=1.0$  kN/m<sup>2</sup> and live load  $Q=1.5$  kN/m<sup>2</sup>, which is a lower load value than prescribed by Eurocode, but a more realistic value for an office programme (Drewniok and Orr, 2019). Whereas dead load is uniformly distributed, live load includes different symmetric and asymmetric load patterns, in a similar approach to Hawkins et al (2020), and as shown in Figure 7. The load combination for the Ultimate Limit State (ULS) is  $1.35(G + G') + 1.5Q$  to check strength (stresses) and stability (buckling), and for the Serviceability Limit State (SLS) is  $1.0(G + G') + 1.0Q$  to check stiffness (deflection), according to BS EN 1992-1-1 Eurocode 2 guidance (British Standards Institution, 2004)

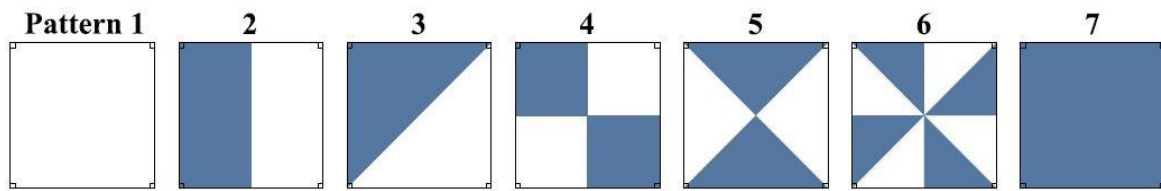


Figure 7 – Live load application (in blue) following various symmetric and asymmetric loading patterns (adapted from Hawkins, 2020).

## 4 Design exploration

The SQUIRREL tool was used to define the final OAK shell geometry, in particular its span and segmentation layout, rib design, three-dimensional shape, and variable thickness, through a design exploration process.

### 4.1 Span and segmentation layout

The span and segmentation layout for the OAK prototype are constrained by the shell's structural behaviour and its fabrication process.

The interfaces between adjacent segments are by design perpendicular to the flow of compressive forces to prevent in-plane sliding failure (Figure 9), which results in an octagonal shape for the central segment, as well as trapezoidal shapes for the edge segments, so that the dominant compression forces prevent the segments from sliding out. Additionally, the segments must fit within a 1.8m-sided square so they can be manufactured on the ACORN adaptive mould. The selected number of segments while respecting these size and alignment constraints was nine (Figure 9). While more segments would enable a longer span, that would increase fabrication time, which was limited by laboratory calendar constraints. Moreover, the layout's symmetry leads to repetition of only three different segment shapes (corner, edge and central) which favours efficiency in manufacturing the segments. Such constraints dictated the shell span, as well as its overall segmentation, and therefore a parametric study was conducted to define a suitable solution for these two features, by tuning the dimensions of the interfaces between segments.

To illustrate the process, consider a square grid layout of three by three 1.8m maximum squares, corresponding to the maximum segment size allowed by the fabrication process, totalling a maximum span of 5.4m (Figure 8a). Despite maximising area efficiency, the adjacency between central and corner segments in such layout is limited to a single point, preventing forces to flow perpendicularly between them. Therefore, the parametric study explored overlaps between maximum squares, through variation of two shape parameters: trapezoidality, and octagonality.

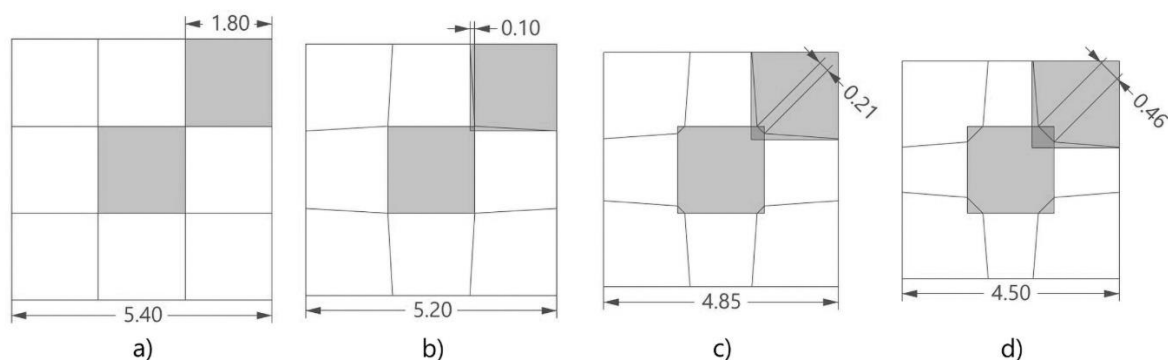


Figure 8 – Variations in segmentation layout (measurements in [m]): a) a square grid maximises area; b) skewed edge segments prevent sliding; c) segmentation layout with smaller central-corner interface; d) segmentation layout selected for OAK.

*Trapezoidality* relates to the length differential between the inner and outer edges of the quadrilateral edge segments, skewing the edge segments in a trapezoidal shape instead of rectangular, and thus preventing in-plane sliding failure. Such differential was set to a minimum of 20mm, split between 10mm for each side (Figure 8b). *Octagonality* relates to the overlap between central and corner segments, changing the shape of the central segment into an octagon. Moving the corner segments towards the shell's centre increases the length of the interface between them, which ensures the continuity of the diagonal ribs and improves force flow. However, it reduces the span of the whole shell.

The final segmentation layout corresponds to a compromise between these two parameters, resulting in a 4.5m span, and an interface between central and corner segments of 460mm, compatible with the 300mm-wide ribs, whose design is presented in a later section (Figure 8d).

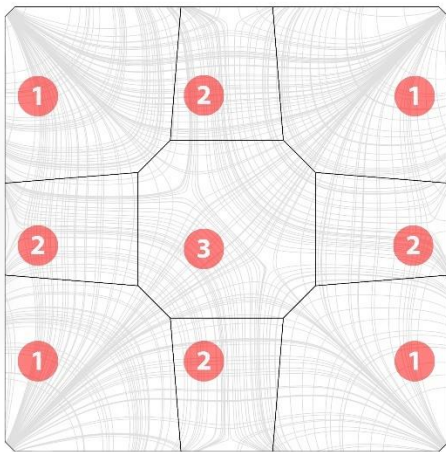


Figure 9 – Network of principal stress lines compared with shell segmentation layout, composed of four identical segments at the corners (1), four identical segments on the edge at mid-span (2) and a single central segment (3).

## 4.2 Three-dimensional shape

Complementing the segmentation layout study, a parametric study was conducted to define the three-dimensional 3D shape of the OAK prototype, as described in Section 3.1.

At this stage of the research, design parameters were constantly changing, often simultaneously, as a result of experimentation in the design framework. Such changes were also informed by insights from developing the fabrication process and building physical prototypes or material tests. Moreover, the computation time of the structural analysis in the design tool was still relatively high, making it difficult to keep repeating parametric studies with new parameters and constraints. Therefore, the value of parametric studies conducted at this stage is in providing insights on the general behaviour of the phenomena they simulate, rather than providing absolute values.














Therefore, rather than finding a definitive shape, this study aimed to determine a subset of good solutions within a pre-determined Design Space, informed by structural performance but mainly driven by the volume of concrete as an early design proxy for embodied carbon, justified by considering a unique material and fabrication process. The domain of the Design Space for this study consists of a set of shell models, whose geometry varies according to shape parameters, coupled with performance indicators for each model, calculated by FEA.

The shape parameters include the ones used in the form-finding process, namely dimensionless edge force and surface stress. Shell thickness was also a varied parameter in this study, which considered shells with the same thickness across its span, while variable thickness was explored only later in the

design process. The performance indicators included those determined earlier to be driving design, namely compression principal stress and buckling load factors, as well as deflection and concrete volume.

For each combination of shape parameters, the minimum thickness was determined that complied with both structural performance conditions, if possible, namely compression stress below 20MPa, tension stress below 4MPa, and buckling load factors above 10, allowing a focus on concrete volume to select the best solutions (Table 1). Rather than prescribing a single optimum solution, the parametric study on the shell's 3D shape provided a range of suitable values for the form-finding parameters.

Table 1 – Parametric study shell designs with structural analysis (compression stress in red, tension stress in blue) and corresponding geometric results (S = Surface stress; E = Edge force; T = Thickness [mm]; V = Volume [m<sup>3</sup>])

S E	0.25	0.50	0.75	1.00
1.00	 T = 37.5 V = 0.950	 T = 35.0 V = 0.882	 T = 35.0 V = 0.881	 T = 35.0 V = 0.880
0.75	 T = 37.5 V = 0.949	 T = 35.0 V = 0.881	 T = 35.0 V = 0.880	 T = 40.0 V = 1.005
0.50	 T = 35.0 V = 0.883	 T = 37.5 V = 0.943	 T = 42.5 V = 1.068	 T = 47.5 V = 1.193
0.25	 T = 42.5 V = 1.070	[not compliant stresses]	[not compliant stresses]	[not compliant stresses]

While this parametric study was conducted for a 5-meter span shell, the parallel segmentation exercise prescribed a smaller span of 4.5m. Nevertheless, the resulting reduction of the design space facilitated the selection of the shell's final shape, which was subsequently determined by a local adjustment of the shape parameters, informed by the integration of a 300mm diameter service duct within the shell's structural depth, running between its edge and the levelled floor (Figure 2).

Consequently, the form-finding parameters were fine tuned to 0.335kN/m for surface stress and 0.915kN for edge force. In fact, the thickness value prescribed at this point was 45mm, corresponding to a 95-percentile compression stress of 5.2MPa and buckling load factor of 9.9, confirming the compliance of the adopted shell shape.

### 4.3 Variable thickness

The definition of 3D shape considered a constant thickness throughout the shell. However, the concentration of stresses near the corners suggests that a variable thickness would further reduce the volume of concrete required.

Therefore, a parametric study was conducted to understand the impact of variable thickness in structural performance. Assuming a quadratic variation between shell thickness at the apex ( $t_{apex}$ ) and at its supports ( $t_{supp}$ ), both input parameters  $t_{apex}$  and  $t_{supp}$  range between 10 and 100mm, while ensuring that  $t_{apex} > t_{supp}$ . The output parameters were the same performance indicators used for exploring constant thickness, namely principal stress, buckling load factors and concrete volume.

Similarly to the building integration objective mentioned earlier, parameters were explored by manual adjustment, with the objective of having the same or better performance compared to the shell design

with constant thickness. In OAK's final design, the thickness increases from 30mm at the apex to 60mm at the supports, where compression forces increase and concentrate towards the columns. This solution resulted in an average thickness of 39mm, i.e., 1/115th of the span, as opposed to ratios around 1/30 for a traditional flat concrete slab (Hawkins et al., 2020). This segmented shell corresponds to a 95-percentile compression stress value of 2.7, and a buckling load factor of 7.3. While buckling is below the defined threshold, this solution corresponds to concrete volume of 0.80m<sup>3</sup>, which is an improvement of 11% relative to the constant thickness option.

#### 4.4 Ribs

The final enhancement to the shell design was the addition of ribs, under the initial assumption that they would improve the shell's stiffness and structural performance (Oval et al., 2019). The rib layout is informed by the superposition of topology optimisation layouts for multiple load cases (Mándoki, 2021). This procedure applied K3D's implementation of Bi-directional Evolutionary Structural Optimisation (BESO) (Huang and Xie, 2010; Preisinger and Tam, 2020) to the variable thickness shell, subjected to each of the asymmetrical load cases presented in Section 3.2. Each load pattern was considered in different horizontal rotations and symmetries (Figure 10). The resulting topology optimisation layouts for each load case were added into a combined thickness optimisation layout with variation of thickness values throughout (Figure 10b).

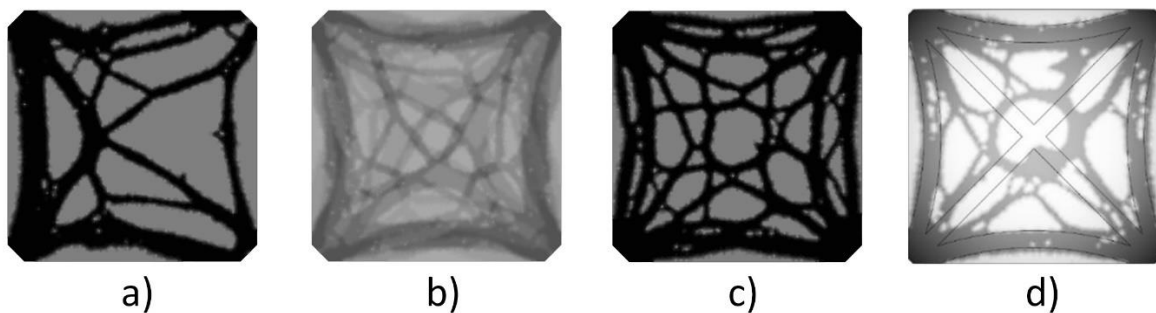


Figure 10 – Thickness optimisation exploration using BESO topology optimisation layouts: a) layout for single rotation of load pattern 2; b) superposition of semi-transparent layouts for multiple rotations of load pattern 2; c) layout for multiple rotations of load pattern 2; d) layout for multiple rotations of all load pattern, compared with final rib layout

While the design of the ribs was informed by the thickness optimisation layout, it was not directly generated by it. In fact, the rib layout corresponds to two crossing diagonals between opposite supports and arches along the edges between adjacent supports, each rib measuring 300mm in width and with an overall thickness of 60mm (Figure 10d). The arcs along the shell edge bear a closer resemblance to the arcs in the BESO optimisation, both in their shape and thickness. On the other hand, the diagonals have a closer resemblance to the force flow diagram (Figure 9), although they could be thought of as the result of the branches identified in the BESO optimisation layout, running between opposite corners, and intersecting around the shell's apex.

Overall thickness along the 300mm-wide ribs has a constant value of 60mm, contrasting more at the 30mm-thick apex than at the supports, where the shell thickness is also 60mm. Thin wide ribs were preferred over thick narrow ones due to constraints identified in preliminary fabrications tests, namely related to the slump of sprayed concrete.

While adding the ribs results in an increase in 4% of concrete volume from the constant thickness shell, it can be considered efficient in comparison to the improvement in terms of structural performance, namely a 33% reduction in 95-percentile compression stress. On the other hand, base thickness could be reduced instead, to save material rather than increase structural performance.

By the end of the design exploration, the shell design was deemed suitable for production. The resulting OAK shell has a span of 4.5m, covering a square area of 20m<sup>2</sup>, and a rise of 590mm, variable thickness from 30mm at the apex to 60mm at the supports, and a set of diagonal and edge ribs 60mm thick and 300mm wide, stiffening the shell. The shell weighed 100kg/m<sup>2</sup>, around 25% of the weight of an equivalent flat slab (Hawkins et al., 2020), resulting in a lighter element, with lesser loads on the columns throughout the building and on the foundations. The structural performance parameters for the final shell design correspond to 95-percentile compression stress of 3.5 MPa and a buckling load factor of 9.6. Table 2 compares performance indicators for the various stages of the shell geometry, after each stage of the design exploration.

Table 2 – Performance results for subsequent shell design stages, considering least favourable load pattern

	Thickness [mm]		Compression stress (95-percentile) [MPa]	Buckling load factors [-]	Concrete volume [m <sup>3</sup> ]
	Apex	Supports			
Constant thickness	45	45	5.2	9.9	0.89
Variable thickness	30	60	2.7	7.3	0.80
Variable thickness + ribs	30	60	3.5	9.6	0.93

## 5 Future research

Future work will be mostly focused on the improvement of the design tool for further use, as informed by the challenges in designing the OAK shell, namely:

- Automating design tasks performed manually in the case of OAK and identified in this paper, but that inform the process of its automation, and integration into the tool, including:
  - Segmentation layout to satisfy fabrication constraints;
  - Determining form-finding shapes compatible with service ducts;
  - Integration of thickness optimisation in rib layout design;
  - Integration of rib layout in variable thickness and width design.
- Optimisation: throughout its development, the tool was used to inform design decisions based on “manual” iterative optimisation processes, such as the aforementioned Design Space Visualisation. Although these broader approaches were useful for understanding the structural behaviour of the shells being designed, it is essential that the tool be coupled with existing optimisation tools, which provide the level of automation expected – and needed – by designers.
- Performance: optimisation processes are constrained by the speed at which the design tool performs structural analysis, which becomes more computationally expensive as models become more detailed. Therefore, further development should strive for making the SQUIRREL tool quicker. This might be achieved by analysing and refactoring existing code, integrating features from plugins into custom components, and ultimately replacing those plugins by faster alternatives.

## 6 Conclusion

This paper presented the design process of the OAK, a prototype segmented concrete thin shell intended for building floors, capable of a 75% reduction in concrete weight and, consequently, reducing its embodied carbon footprint. The design process was driven by SQUIRREL, a computational design tool developed with the purpose of designing not only the OAK prototype but a wide spectrum of designs, and whose main objective is to simplify that process through design automation.

Implemented as a parametric modelling framework, it combines the potential of form-finding, finite element analysis, fabrication constraints, and design space exploration and visualisation.

SQUIRREL was used for various aspects that determined the shell design, including segmentation layout informed by fabrication constraints, three-dimensional shape informed by structural performance and building integration, variable thickness, and ribs to improve structural performance. Such a design process was crucial for the development of the design tool.

To have an impact on the industry, further research is needed to demonstrate the applicability of the ACORN shells in practice, and answer questions raised during its development regarding comfort, insulation, and fire safety. These issues will impact the design of the proposed segmented thin shells, and consequently steer the development of the ACORN design tool, which to date has been mostly driven by structural performance and fabrication constraints. This will enable ACORN to live up to its original commitment: to deliver an integrated end-to-end digital process for the design and manufacture of more sustainable concrete building elements.

## 7 Acknowledgements

The Automating Concrete Construction (ACORN) research project was funded by UKRI through the ISCF Transforming Construction programme, grant number EP/S031316/1. The authors wish to thank the rest of the ACORN team for their support, as well as the industrial project partners and affiliates for their feedback.

## 8 References

- Anderson, J., Moncaster, A., 2020. Embodied carbon of concrete in buildings, Part 1: analysis of published EPD. *Buildings and Cities* 1, 198–217. <https://doi.org/10.5334/bc.59>
- Bannister, T.C., 1968. The Roussillon Vault: The Apotheosis of a “Folk” Construction. *Journal of the Society of Architectural Historians* 27, 163–175. <https://doi.org/10.2307/988500>
- Bauer, A., Längst, P., Wüchner, R., Bletzinger, K.-U., 2017. *Isogeometric Analysis for Modeling and Simulation of Building Processes*.
- Bletzinger, K.-U., Ramm, E., 1999. A General Finite Element Approach to the form Finding of Tensile Structures by the Updated Reference Strategy. *International Journal of Space Structures* 14, 131–145. <https://doi.org/10.1260/0266351991494759>
- Block, P., Calvo Barentin, C., Ranaudo, F., Paulson, N., 2020. Imposing Challenges, Disruptive Changes: Rethinking the floor slab, in: Ruby, I., Ruby, A. (Eds.), *The Materials Book*. Ruby Press, pp. 214–219.
- Block, P., DeJong, M.J., Davis, L.K., Ochsendorf, J., 2010. Tile vaulted systems for low-cost construction in Africa. *Journal of the African Technology Development Forum (ATDF)* 7, 4–13.
- British Standards Institution, 2004. BS EN 1992-1-1 Eurocode 2: Design of concrete structures - Part 1-1: General rules and rules for buildings.
- Brown, N.C., Jusiega, V., Mueller, C.T., 2020. Implementing data-driven parametric building design with a flexible toolbox. *Autom Constr* 118, 103252. <https://doi.org/10.1016/J.AUTCON.2020.103252>

- Broyles, J.M., Shepherd, M.R., Brown, N.C., 2022. Design Optimization of Structural–Acoustic Spanning Concrete Elements in Buildings. *Journal of Architectural Engineering* 28, 04021044. [https://doi.org/10.1061/\(ASCE\)AE.1943-5568.0000520](https://doi.org/10.1061/(ASCE)AE.1943-5568.0000520)
- De Wolf, C., Ramage, M., Ochsendorf, J., 2016. Low carbon vaulted masonry structures. *Journal of the International Association for Shell and Spatial Structures* 57, 275–284. <https://doi.org/10.20898/j.iass.2016.190.854>
- Debney, P., 2020. Computational engineering. Institution of Structural Engineers (Great Britain).
- Department for Business Innovation & Skills, 2010. Estimating the amount of CO2 emissions that the construction industry can influence - Supporting material for the Low Carbon Construction IGT Report.
- Drewniok, M.P., Orr, J., 2019. Minimising energy in construction: Demonstrating floor loading.
- Goldbach, A.K., Bauer, A.M., Wüchner, R., Bletzinger, K.U., 2020. CAD-Integrated Parametric Lightweight Design With Isogeometric B-Rep Analysis. *Front Built Environ* 6, 44. <https://doi.org/10.3389/fbuil.2020.00044>
- Guastavino, R., 1892. *Essay on the Theory and History of Cohesive Construction: Applied Especially to the Timbrel Vault*, 1st ed. Ticknor, New York City.
- Hawkins, W., Orr, J., Ibell, T., Shepherd, P., 2020. A design methodology to reduce the embodied carbon of concrete buildings using thin-shell floors. *Eng Struct* 207, 110195. <https://doi.org/10.1016/j.engstruct.2020.110195>
- Hawkins, W.J., 2020. *Thin-shell Concrete Floors for Sustainable Buildings (Doctor of Philosophy (PhD))*. University of Cambridge. <https://doi.org/10.17863/CAM.45976>
- Hawkins, W.J., Herrmann, M., Ibell, T.J., Kromoser, B., Michaelski, A., Orr, J.J., Pedreschi, R., Pronk, A., Schipper, H.R., Shepherd, P., Veenendaal, D., Wansdrong, R., West, M., 2016. Flexible formwork technologies - a state of the art review. *Structural Concrete* 17, 911–935. <https://doi.org/10.1002/suco.201600117>
- Huang, X., Xie, Y.M., 2010. Evolutionary Topology Optimization of Continuum Structures: Methods and Applications. *Evolutionary Topology Optimization of Continuum Structures: Methods and Applications*. <https://doi.org/10.1002/9780470689486>
- Längst, P., Bauer, A.M., Michalski, A., Lienhard, J., 2017. The Potentials of Isogeometric Analysis Methods in Integrated Design Processes, in: *International Association for Shell and Spatial Structures (IASS) Symposium*. International Association for Shell and Spatial Structures (IASS).
- Liew, J.Y.R., Chua, Y.S., Dai, Z., 2019. Steel concrete composite systems for modular construction of high-rise buildings. *Structures* 21, 135–149. <https://doi.org/10.1016/J.ISTRUC.2019.02.010>
- Mándoki, S., 2021. Automating Concrete Construction: Development of a topology optimised shell.
- Medwadowski, S.J., 2004. Buckling of Concrete Shells: An Overview. *Journal of the International Association for Shell and Spatial Structures* 45, 51–63.
- Nuh, M., Oval, R., Orr, J., 2022. ARCS: Automated Robotic Concrete Spraying for the Fabrication of Variable Thickness Doubly Curved Shells 267–273. [https://doi.org/10.1007/978-3-031-06116-5\\_40](https://doi.org/10.1007/978-3-031-06116-5_40)



- Ochsendorf, J.A., Freeman, M., 2014. *Guastavino vaulting: the art of structural tile*. Princeton Architectural Press.
- Opon, J., Henry, M., 2019. An indicator framework for quantifying the sustainability of concrete materials from the perspectives of global sustainable development. *J Clean Prod* 218, 718–737. <https://doi.org/10.1016/J.JCLEPRO.2019.01.220>
- Orr, J.J., Darby, A.P., Ibell, T.J., Evernden, M.C., Otlet, M., 2011. Concrete structures using fabric formwork. *The Structural Engineer* 89, 20–26.
- Oval, R., Costa, E., Nuh, M., Thomas-McEwen, D., Orr, J., Shepherd, P., 2021. A path towards the off-site automated fabrication of segmented concrete shells for building slabs, in: *Proceedings of the IASS Annual Symposium 2020/21 and the 7th International Conference on Spatial Structures: Inspiring the Next Generation*.
- Oval, R., Nuh, M., Costa, E., Madyan, O.A., Orr, J., Shepherd, P., 2023. A prototype low-carbon segmented concrete shell building floor system. *Structures* 49, 124–138. <https://doi.org/10.1016/j.istruc.2023.01.063>
- Oval, R., Rippmann, M., Mesnil, R., van Mele, T., Baverel, O., Block, P., 2019. Feature-based topology finding of patterns for shell structures. *Autom Constr* 103, 185–201. <https://doi.org/10.1016/J.AUTCON.2019.02.008>
- Preisinger, C., 2013. Linking Structure and Parametric Geometry. *Architectural Design* 83, 110–113. <https://doi.org/10.1002/ad.1564>
- Preisinger, C., Tam, M., 2020. The official guide to using Karamba3D 1.3.3 [WWW Document]. URL <https://manual.karamba3d.com/> (accessed 11.4.21).
- Reitinger, R., Ramm, E., 1995. Buckling and imperfection sensitivity in the optimization of shell structures. *Thin-Walled Structures* 23, 159–177. [https://doi.org/10.1016/0263-8231\(95\)00010-B](https://doi.org/10.1016/0263-8231(95)00010-B)
- Robert Hooke, 1675. *A description of helioscopes and some other instruments*. London.
- Rutten, D., 2009. *Grasshopper*.
- Shepherd, P., Orr, J., Ibell, T., Parlikad, A., Spadea, S., 2019. ACORN: Automating Concrete Construction [WWW Document]. URL <https://automated.construction/> (accessed 4.13.21).
- United Nations, 2015. *Transforming Our World: The 2030 Agenda for Sustainable Development*.